

Reaction Dynamics of the 4-Methylphenyl Radical (p-Tolyl) with 1,2-Butadiene (1-Methylallene) – Are Methyl Groups purely Spectators?

Ralf I. Kaiser,* Beni B. Dangi, Tao Yang, Dorian S. N. Parker

Department of Chemistry, University of Hawai'i at Manoa, Honolulu, HI 96822, USA

Tel: 808-956-5731

E-mail: ralfk@hawaii.edu

Alexander M. Mebel*

Department of Chemistry and Biochemistry, Florida International University, Miami, FL 33199, USA

Tel: 305-348-1945

E-mail: mebela@fiu.edu

Abstract

The reactions of the 4-tolyl radical ($C_6H_4CH_3$) and of the D7-4-tolyl radical ($C_6D_4CD_3$) with 1,2-butadiene (C_4H_6) have been probed in crossed molecular beams under single collision conditions at a collision energy of about 54 kJ mol^{-1} and studied theoretically using ab initio G3(MP2,CC)//B3LYP/6-311G** and statistical RRKM calculations. The results show that the reaction proceeds via indirect scattering dynamics through the formation of a van-der-Waals complex followed by the addition of the radical center of the 4-tolyl radical to the C1 or C3 carbon atoms of 1,2-butadiene. The collision complexes then isomerize by migration of the tolyl group from the C1 (C3) to the C2 carbon atom of the 1,2-butadiene moiety. The resulting intermediate undergoes unimolecular decomposition via elimination of a hydrogen atom from the methyl group of the 1,2-butadiene moiety through a rather loose exit transition state leading to 2-para-tolyl-1,3-butadiene (**p4**), which likely presents the major reaction product. Our observation combined with theoretical calculations suggest that one methyl group (at the phenyl group) acts as a spectator in the reaction, whereas the other one (at the allene moiety) is actively engaged in the underlying chemical dynamics. On the contrary to the reaction of the phenyl radical with allene, which leads to the formation of indene, the substitution of a hydrogen atom by a methyl group in allene essentially eliminates the formation of bicyclic PAHs such as substituted indenenes in the 4-tolyl plus 1,2-butadiene reaction.

Keywords: gas-phase chemistry, physical-organic chemistry, bimolecular reaction, reaction mechanism, combustion.

1. Introduction

Polycyclic aromatic hydrocarbons (PAHs) and related aromatic compounds such as ionized and substituted PAHs are proposed to be ubiquitous in extraterrestrial environments.¹ Photochemical reactions of these compounds on ice coated interstellar nanoparticles produce organic compounds such as alcohols, ethers, and even RNA-relevant nitrogen bases² linking them to the origin of life on Earth. In addition to their possible role in biogenesis, these compounds make up to 30 % of the cosmic carbon and have been suggested as the carriers of both the diffuse interstellar bands (DIBs)³ and the unidentified infrared (UIR)⁴ emission bands. On Earth, mostly due to the anthropogenic activities, PAHs are formed by pyrolysis and incomplete combustion of organic matter (fossil fuel, bio fuel) and are considered acute atmospheric and surface pollutants due to their toxic effects as mutagens and carcinogens. Hence the formation mechanisms of PAHs are of particular interest to the combustion and astrochemistry communities due to their critical role as reaction intermediates in soot growth⁵ and also in the formation of interstellar dust particles.⁶

Flame tests are the most popular investigatory techniques to probe the formation of PAHs and their growth mechanisms in hydrocarbon combustion.^{7, 8} These studies often utilize photoionization mass spectrometry to monitor the mass growth process and to identify the structural isomers formed based on the photoionization efficiency curves.⁹ The mass growth processes are believed to start at the molecular level with the synthesis of the very first mono cyclic structures, such as the phenyl radical (C_6H_5) and benzene (C_6H_6) suggested to be the rate determining steps¹⁰⁻¹² and reach particulate size up to several tens of nanometers.¹³⁻¹⁶ The formation of aromatics and substituted aromatics containing five- and six-member rings is of particular interest^{9, 17, 18} since these molecules play an important role in reaction mechanisms governing the

mass growth of higher, potentially non-planar PAHs and soot in combustion flames.^{7, 8} Simple PAH species with five and six-membered rings including indene and fluorine are abundant in flames and may be involved in the further growth of the PAHs and subsequently larger non-planar structures such as corannulene and ultimately to fullerenes and soot.¹¹ Even though flame studies depict the actual combustion like conditions, it is often difficult to draw conclusions from these experiments due to the occurrences of complex parallel and sequential multiple chemical reactions. Hence, only detailed investigations of successive bimolecular reactions at the microscopic level can help fully understand the involved reaction dynamics and kinetics.

Phenyl radical reactions are one of the extensively studied bimolecular reactions with unsaturated hydrocarbon molecules leading to PAHs.¹⁹ Indene (C_9H_8),²⁰ naphthalene ($C_{10}H_8$),²¹ as well as 1,4-dihydronaphthalene ($C_{10}H_{10}$)²² were found to be synthesized via bimolecular reactions of the phenyl radical (C_6H_5) with allene/methylacetylene (C_3H_4), vinylacetylene (C_4H_4), and 1,3-butadiene (C_4H_6), respectively. The related methyl-substituted aromatic radical - methylphenyl ($C_6H_4CH_3$) - represents the simplest alkyl-substituted phenyl radical; this species can be seen as an isomer of the benzyl radical ($C_6H_5CH_2$), which is abundant in combustion flames²³ as probed by Zhang et al.. Due to their importance as reaction intermediates in hydrocarbon growth and soot formation, the potential energy surfaces (PESs) of the C_7H_7 radicals - benzyl ($C_6H_5CH_2$), o-, m-, and p-tolyl (or 2-, 3-, and 4-tolyl) ($C_6H_4CH_3$), and cycloheptatrienyl (C_7H_7) - have been explored extensively.^{23, 24} Experiments carried out under bulk conditions showed that the reaction of the C_7H_7 radical with the methyl radical produces styrene (C_8H_8) and molecular hydrogen.²⁵ However, with the exception of the reaction of 4-tolyl (p-tolyl) radicals with vinylacetylene (C_4H_4), which leads to the formation of 2-methylnaphthalene,²⁶ reactions of *any* C_7H_7 isomer with unsaturated hydrocarbons under single collision conditions

have been elusive. In this paper, we report on the reaction of the 4-methylphenyl (4-tolyl) radical with 1,2-butadiene ($\text{H}_2\text{CCCH}(\text{CH}_3)$) and elucidate to what extent substituted PAHs can be formed under single collision conditions. The results of this study are also compared to the reaction of the ‘non-substituted counterparts’, i.e. of the phenyl radical with allene studied earlier in our laboratory²⁰ ultimately revealing if the methyl group acts purely as a spectator or is actively involved in the reaction dynamics.

2. Methods

2.1. Experimental and Data Analysis

The reactions of the 4-tolyl radical ($\text{C}_6\text{H}_4\text{CH}_3$) and of the D7-tolyl radical ($\text{C}_6\text{D}_4\text{CD}_3$) with 1,2-butadiene (C_4H_6) were carried out in a crossed molecular beam machine under single collision conditions.²⁷ Briefly, a supersonic molecular beam of the (D7-) 4-tolyl radicals seeded in helium (99.9999%; Airgas Gaspro) at fractions of about 0.1 % was generated via photodissociation of 4-chlorotoluene ($\text{C}_6\text{H}_4\text{CH}_2\text{Cl}$; Sigma-Aldrich) and D7-4-chlorotoluene ($\text{C}_6\text{D}_4\text{CD}_2\text{Cl}$) in the primary source chamber. The seeded precursor beam was prepared by passing 1.8 atm helium through (D7-) 4-chlorotoluene in a stainless steel bubbler and releasing this mixture into the primary source chamber via a pulsed valve (Piezo Disk Translator; Physik Instrumente) operating with a 0.96 mm nozzle at 120 Hz, 80 μs pulse width, and about -450 V pulse amplitude. The (D7-) 4-chlorotoluene was photodissociated by a 193 nm laser beam emitted from a Lambda Physik Compex 110 Excimer laser operated at 60 Hz repetition rate and pulse energy of 12 ± 2 mJ. The laser beam was focused by a 1.5 m quartz focus lens to 4×1 mm before it intercepted the molecular beam perpendicularly 1 mm downstream of the nozzle. A four-slot chopper wheel was installed after the skimmer and selected a segment of the radical beam. This segment of the radical beam crossed perpendicularly a secondary, pulsed molecular

beam of 1,2-butadiene (98%; ChemSampCo) released by a second pulsed valve at a frequency of 120 Hz, 80 μs pulse width, and -400 V pulse amplitude (Table 1). The delay times of the pulsed valves and the laser were synchronized in order to obtain the best signal-to-noise ratios of the reactive scattering products. A photodiode mounted on top of the chopper wheel provided the time zero trigger; the primary and secondary pulsed valves were triggered at 1872 μs and 1822 μs respectively, after the time zero. The excimer laser was fired with a delay time of 180 μs with respect to the primary pulsed valve. It is important to note that the 4-tolyl radical can, in principle, isomerize to 3-tolyl and/or 2-tolyl and also to the thermodynamically more stable benzyl radical ($\text{C}_6\text{H}_5\text{CH}_2$). However, even the lowest energy barrier for such isomerization would require 180 kJ mol^{-1} ,²⁸ which is too high for the available energy in our experimental conditions (single photon dissociation). Photodissociation experiments similar to our conditions at 193 nm have been reported in the literature.^{29, 30} which measure two major channels with translational energies [67 kJ mol^{-1} (31%) and 130 kJ mol^{-1} (60%)] dissipating in the 4-tolyl radical.³⁰ Only about 2 kJ mol^{-1} of internal energy exits in the molecular beam (at 200-300 K) making it insignificant factor. Hence, by subtracting these translational energies and C-Cl bond dissociation energy (407 kJ mol^{-1})³⁰ from the photon energy, we obtain available energies as 146 kJ mol^{-1} (31%) and 83 kJ mol^{-1} (60%). The barriers for isomerization among 2-, 3- and 4-methylphenyl radicals are estimated to be about 260 kJ mol^{-1} .²⁸ Hence, this barrier is energetically not accessible in our experiments.

The fully deuterated isotope of the p-tolyl radical, C_7D_7 , was used to identify the origin of the leaving hydrogen atom in the reaction, i.e., to elucidate whether the leaving hydrogen atom originated from the p-tolyl radical and/or 1,2-butadiene. Synthesis of the D7-4-chlorotoluene started from commercially available para-toluidine. The starting material was deuterated using

palladium-carbon (Pd/C) and platinum-carbon (Pt/C) catalysts and deuterium oxide in an autoclave at 190°C for 96 h. This deuteration procedure was repeated three times to obtain the labeled compound. Deuteration progress was monitored with ^{13}C carbon NMR and mass spectrometry. Subsequently, the chloro compound was obtained by converting the toluidine to its diazonium salt and substitution of the diazo group with chloride in a Sandmeyer type reaction.³¹

The reactively scattered products were detected using a triply differentially pumped time-of-flight (TOF) mass spectrometer after electron-impact ionization (80 eV, 2 mA) and mass filtering by a quadrupole filter (QC 150, Extrel) at pressures of a few 10^{-12} torr. The detector was rotated within the plane defined by the two reactant beams to collect the TOF spectra at various laboratory angles. We recorded up to 5×10^5 TOF spectra per laboratory angle, integrated and normalized angular-resolved TOF spectra, and extracted the product angular distribution at a defined mass-to-charge ratio in the laboratory (LAB) frame. Information on the chemical dynamics was obtained by fitting the TOF spectra and the laboratory angular distribution (LAB) by using a forward-convolution routine. This routine initially assumes an angular distribution, $T(\theta)$, and a translational energy distribution, $P(E_T)$, in the center-of-mass (CM) reference frame. TOF spectra and the LAB distributions were then calculated from these CM functions until the best fits were obtained by iteratively refining the adjustable parameters in the center-of-mass system within the experimental error limits in the laboratory frame. We obtained the product flux contour map, $I(\theta, u) = T(\theta) \times P(u)$, which represents the intensity of the reactive scattering products (I) as a function of the center-of-mass scattering angle (θ) and the product velocity (u). This plot yields an ‘image’ of the chemical reaction.

2.2. Computational Details

Geometries of various intermediates, transition states, and products involved in the reaction of the 4-tolyl radical with 1,2-butadiene were optimized at the hybrid density functional B3LYP level of theory with the 6-311G(d,p) basis set.³² Vibrational frequencies and zero-point vibrational energy (ZPE) were obtained using the same B3LYP/6-311G (d,p) approach. The optimized geometries of all species were then used in single-point calculations to refine energies at the G3(MP2,CC)//B3LYP level of theory, which is modification^{33, 34} of the original Gaussian 3 (G3) scheme.³⁵ The final energies at 0 K were obtained using the B3LYP optimized geometries and ZPE corrections according to the following equation:

$$E_0[\text{G3(MP2,CC)}] = E[\text{CCSD(T)/6-311G(d,p)}] + \Delta E_{\text{MP2}} + E(\text{ZPE}),$$

where $\Delta E_{\text{MP2}} = E[\text{MP2/G3large}] - E[\text{MP2/6-311G(d,p)}]$ is the basis set correction and $E(\text{ZPE})$ is the zero-point energy. $\Delta E(\text{SO})$, a spin-orbit correction, and $\Delta E(\text{HLC})$, a higher level correction, from the original G3 scheme were not included, as they are not expected to make significant contributions into relative energies. The accuracy of the G3(MP2,CC)//B3LYP/6-311G** relative energies is normally within 10 kJ mol⁻¹. Also, B3LYP optimized geometries of hydrocarbon molecules and radicals normally provide accuracy within 0.01-0.02 Å for bond lengths and 1-2° for bond and torsional angles.³³⁻³⁵ The GAUSSIAN 09³⁶ and MOLPRO 2010³⁷ programs were used for the ab initio calculations.

RRKM theory³⁸ was utilized to compute energy-dependent reaction rate constants of unimolecular reaction steps following the formation of initial adducts under single-collision conditions. Available internal energy for each species, including intermediates and transition states, was taken as the energy of chemical activation plus the collision energy assuming that the latter is dominantly converted into the internal vibrational energy. Harmonic approximation was used for calculations of the density and number of states required to compute the rate constants,

except for the methyl group rotations, which were treated as free rotors. Phenomenological first-order rate equations were then solved within the steady-state approximation using the RRKM rate constants to evaluate product branching ratios for decomposition of various initial reaction adducts formed by the addition of 4-tolyl radical to 1,2-butadiene.

3. Experimental Results

3.1. Laboratory Data

We recorded reactive scattering signal at mass-to-charge ratios, m/z , of 144 ($C_{11}H_{12}^+$), 143 ($C_{11}H_{11}^+$), and 142 ($C_{11}H_{10}^+$) for the reaction of the 4-tolyl radical (C_7H_7) with 1,2-butadiene (C_4H_6). The TOF spectra at lower mass-to-charge ratios of 143 and 142 were superimposable after scaling with the ones obtained at $m/z = 144$. Therefore, we can conclude that signals at $m/z = 143$ and 142 originate from the dissociative ionization of the $C_{11}H_{12}$ product in the electron impact ionizer of the detector. Consequently, we recorded the TOF spectra at $m/z = 144$ ($C_{11}H_{12}^+$; Figure 1a/c), i.e. the m/z value with the best signal-to-noise ratio, and obtained the corresponding LAB angular distribution (Figure 2a/c). Therefore, we can conclude that in the reaction of the phenyl radical with 1,2-butadiene, at least one hydrogen emission pathway is open. Since both the 4-tolyl radical and the 1,2-butadiene molecule can lose a hydrogen atom, we also explored to what extent the hydrogen atom is emitted from the 1,2-butadiene reactant and/or from the 4-tolyl radical. Therefore, we conducted the crossed beam reaction of the D7-tolyl radical (C_7D_7 ; 98 amu) with 1,2-butadiene (C_4H_6 ; 54 amu) as well (Figures 1b/d and 2b/d). Data recorded at $m/z = 151$ ($C_{11}D_7H_5^+$) were fit with a single channel of product mass combination of 1 amu and 151 amu. Therefore, we can conclude that the hydrogen atom is lost at least from the 1,2-butadiene reactant. Scaling for the intensities of the primary radical beams, the scaled intensities of the TOF data of the atomic hydrogen losses at $m/z = 144$ ($C_{11}H_{12}^+$) and $m/z = 151$ ($C_{11}D_7H_5^+$) are

within about 5 - 10 %. This finding proposes that the hydrogen atom is lost predominantly from the 1,2-butadiene reactant. Finally, since both of the reactants contain a methyl group, we attempted to record data for possible methyl loss channel as detected in the crossed beam reactions of the phenyl/D5-phenyl radical with propene (CH_3CHCH_2)³⁹ and of the boron monoxide radical (BO) with methylacetylene (CH_3CCH)⁴⁰ and with dimethylacetylene (CH_3CCCH_3).⁴¹ Due to kinematic constraints, estimated up to 10-15% relative to H loss, no appreciable signal for methyl loss channel was detected.

3.2 Center-of-Mass Frame

Having concluded that the hydrogen loss originates (mainly) from the 1,2-butadiene molecule, we can now extract information on the underlying reaction dynamics by converting the laboratory data into the CM reference frame (Figure 3) by utilizing parameterized center-of-mass functions. For the 4-tolyl plus 1,2-butadiene and D7-4-tolyl plus 1,2-butadiene systems, the TOF spectra and LAB angular distributions could be fit with a single channel of a mass combination of 144 amu ($\text{C}_{11}\text{H}_{12}$) plus 1 amu and 151 amu ($\text{C}_{11}\text{D}_7\text{H}_5$) plus 1 amu (H), respectively. These fits were relatively insensitive to the high energy cutoffs and to the distribution maxima of the center-of-mass translational energy distributions. For both systems, best fits were obtained with translational energy distributions, which can be extended up to $128 \pm 22 \text{ kJ mol}^{-1}$ (Figure 3, upper left) and even $200 \pm 25 \text{ kJ mol}^{-1}$ (Figure 3, lower left). Since for those products born without internal excitation the high-energy cutoff represents the sum of the absolute reaction energy and the collision energy, we determined reaction energies between $74 \pm 25 \text{ kJ mol}^{-1}$ and $146 \pm 29 \text{ kJ mol}^{-1}$. In addition, the translational energy distributions depict distribution maxima between 25 and 50 kJ mol^{-1} . We would like to stress that the reaction energies of both systems are not well defined: fits of the TOF (Fig. 1) and LAB data (Fig. 2) can be essentially obtained

for any reaction energy between 74 kJ mol^{-1} and 146 kJ mol^{-1} . Finally, we attempted to fit the laboratory data with lower reaction exoergicities down to $35 \pm 10 \text{ kJ mol}^{-1}$ and $26 \pm 10 \text{ kJ mol}^{-1}$, i.e. the reaction energies associated with the formation of the **p1** (1-para-tolyl-1,2-butadiene) and **p2** (1-para-tolyl-2-butyne) isomers, respectively (Figures 4 and 5). As evident from the fits, the laboratory data could not be reproduced with such low reaction energies since the simulated laboratory angular distributions were – due to the much lower reaction exoergicity – effectively narrower compared to the experimental data (Figure 2). Therefore, based on the energetics we can conclude that the reaction exoergicities of the 4-tolyl with 1,2-butadiene and D7-4-tolyl with 1,2-butadiene systems range between $74 \pm 25 \text{ kJ mol}^{-1}$ and $146 \pm 29 \text{ kJ mol}^{-1}$.

We also obtained additional information on the chemical dynamics from the center-of-mass angular distributions $T(\theta)$ (Figure 3b and 3d). Both $T(\theta)$ s peak around 90° and extend over the complete angular range from 0° to 180° . This finding indicates indirect reaction dynamics via the formation of bound amu $\text{C}_{11}\text{H}_{13}/\text{C}_{11}\text{D}_7\text{H}_6$ intermediate(s).⁴² Further, the maxima at 90° suggest that the hydrogen atom is ejected from the decomposing intermediates almost perpendicularly to the rotational plane of the complex, i. e. nearly parallel to the total angular momentum vector. Finally, the slight asymmetry around 90° depicts an enhanced flux in the forward hemisphere with respect to the 4-tolyl radical beam while the second set shows the perfect symmetry. The ratios of intensities at poles, $I(180^\circ)/I(0^\circ)$, are about 0.7 to 1.0, which allows us to conclude that the lifetime(s) of the bound $\text{C}_{11}\text{H}_{13}/\text{C}_{11}\text{D}_7\text{H}_6$ intermediate(s) is comparable to their rotational period(s).⁴³

4. Theoretical Results

In the case of polyatomic systems, it is always valuable to merge the crossed molecular beam data with the electronic structure and statistical calculations (Figures 4 and 5; Table 2. Our calcu-

lations predict twelve feasible reaction channels forming products **p1** to **p12** via atomic hydrogen and methyl loss pathways in overall exoergic reactions (14 kJ mol⁻¹ to 196 kJ mol⁻¹). Here, the reaction of the phenyl radical with 1,2-butadiene is initiated by the formation of a van-der-Waals complex **i0**, which is slightly bound by 7 kJ mol⁻¹ with respect to the separated reactants. This complex can isomerize via addition of the 4-tolyl radical with its radical center to the C1, C2, and C3 carbon atoms of the 1,2-butadiene reactant leading to the formation of intermediates **i1** (Figure 4), **i2** (Figure 4 and 5), and **i3** (Figure 5), respectively; these collision complexes are bound by 157, 258, and 156 kJ mol⁻¹, respectively. Note that these pathways involve moderate barriers to addition of magnitude 8-9 kJ mol⁻¹, which are slightly above the energies of the separated reactants. However, within the accuracy of our calculations of ± 10 kJ mol⁻¹, this barrier might drop below the energies of the separated reactants possibly resulting in a *submerged* barrier as seen for the phenyl – vinylacetylene,²¹ 4-tolyl – vinylacetylene,²⁶ and phenyl – 1,3-butadiene⁴⁴ systems. These intermediates can either undergo unimolecular decomposition by eliminating an atomic hydrogen and/or a methyl group or isomerize prior to further decomposition. In detail, intermediate **i1** can emit a hydrogen atom from the C1 or C3 carbon atom of the 1,2-butadiene moiety forming **p1** (1-para-tolyl-1,2-butadiene) and **p2** (1-para-tolyl-2-butyne), respectively; a methyl loss from the C3 carbon atom yields **p3** (1-para-tolyl-1-methylacetylene). The overall reactions are slightly exoergic (26 to 55 kJ mol⁻¹) and hold tight exit transition states of 22 to 34 kJ mol⁻¹ with latter associated to a higher-energy exit transition state due to the methyl group loss. Further, **i2** can emit a hydrogen atom from the methyl group of the 1,2-butadiene moiety yielding **p4** (2-para-tolyl-1,3-butadiene) in an overall exoergic reaction (74 kJ mol⁻¹) via relatively loose transition state and a low exit barrier of 7 kJ mol⁻¹. Noteworthy, we could not locate a transition state for the H loss from **i2** to **p4** at our standard

B3LYP/6-311G(d,p) level of theory for geometry optimization but this transition state was found using MP2/6-311G(d,p) and CCSD/6-31G(d) methods. Finally, intermediate **i3** can eliminate a methyl group (from C3 carbon atom of the 1,2-butadiene moiety) or a hydrogen atom (from C3 or C1 carbon atom of the 1,2-butadiene moiety), leading to **p8** (para-tolyl-allene), **p9** (1-para-tolyl-1-methylallene), and **p10** (3-para-tolyl-1-butyne), respectively.

Besides the methyl and hydrogen loss pathways of the initial collision complexes, **i1** and **i3** were found to isomerize. Intermediate **i1** undergoes hydrogen migration from the C2 carbon atom of the tolyl group to the C2 carbon atom of the 1,2-butadiene moiety yielding **i4**. Alternatively, **i1** can isomerize via ring closure to the bicyclic intermediate **i5**; considering the inherent barriers, the isomerization of **i1** to **i5** should be preferential. The latter is metastable and only has to overcome a barrier of 3 kJ mol⁻¹ to yield **i2**, whereas **i4** undergoes a ring-closure to **i6**. Intermediate **i6** can lose a hydrogen atom yielding **p5** (3,6-dimethylindene) and/or **p6** (1,7-dimethylindene) or a methyl group to yield **p7** (6-methylindene). Finally, we have to consider potential isomerization pathways of **i3**. Similar to **i1**, **i3** can isomerize to **i2** by formal migration of the tolyl group involving the carbon-carbon double bond via a metastable intermediate **i8**. Also, a hydrogen shift from the C2 atom of the tolyl to the 1,2-butadiene moiety yields **i7**, which eventually ring-closes to **i9**. The latter can either lose a hydrogen atom forming dimethyl substituted indenenes (**p11**, **p12**) or fragments via methyl loss to singly methyl substituted indene (**p7'**). In summary, considering the inherent barriers to isomerization, the intermediates **i1** (**i3**) either decompose to **p1** (**p9**), **p2** (**p10**), and/or **p3** (**p8**) or isomerize eventually to **i2** with the latter emitting atomic hydrogen to form **p4** (2-para-tolyl-1,3-butadiene). Although the dimethyl-substituted indenenes (**p5**, **p6**, **p11**, **p12**) and methylindene (**p7**, **p7'**) can be formed, their production is less feasible due to the higher barriers along the **i1** (**i3**) → **i4** (**i7**) → **i6** routes as compared

to **i1 (i3)** → **i5 (i8)** → **i2**. For completeness, it should be also noted that the initial van-der-Waals complex **i0** can also undergo intramolecular hydrogen transfer, i.e. essentially a hydrogen abstraction from the C1, C3, and/or methyl group by the para tolyl radical (Figure 4) overcoming barriers of 11-16 kJ mol⁻¹ relative to the initial reactants.

4. Discussion

The underlying potential energy surfaces (Figures 4 and 5) are quite complex, and we are merging now the theoretical predictions with the experimental data from the crossed beam experiments. Let us summarize the results first (R1-R5).

(R1) The reactions of the 4-tolyl radical with 1,2-butadiene and the D7-4-tolyl radical with 1,2-butadiene lead to the formation of C₁₁H₁₂ (144 amu) and C₁₁D₇H₅ (151 amu) via atomic hydrogen ejection.

(R2) No methyl loss channel was observed in these experiments.

(R3) The experiments with D7-4-tolyl radicals with 1,2-butadiene reaction system exhibit that the hydrogen is emitted mainly (up to 90 %) from the 1,2-butadiene reactant, but not from the 4-tolyl radical.

(R4) The reactions follow indirect scattering dynamics via complex formation with lifetimes close to their rotation periods.

(R5) The fits were relative insensitive to the reaction energies and can account for reaction exoergicities between 74 ± 25 kJ mol⁻¹ and 146 ± 29 kJ mol⁻¹.

First, let us analyze the reaction energies. The experimentally determined reaction energies of 74 ± 25 kJ mol⁻¹ and 146 ± 29 kJ mol⁻¹ for the atomic hydrogen loss can be rationalized by the

synthesis of methyl-disubstituted indenenes (**p5**, **p6**, **p11**, **p12**) ($\Delta_{\text{R}}G = -154 \pm 10 - 167 \pm 10 \text{ kJ mol}^{-1}$) via intermediates **i6/i9** and/or for the synthesis of **p4** ($\Delta_{\text{R}}G = -74 \pm 10 \text{ kJ mol}^{-1}$) through unimolecular decomposition of intermediate **i2**. Based on the experimental energetics and a comparison with the theoretical data alone, we cannot conclude which of these products is formed. However, the failed detection of the methyl group loss channel might assist us to narrow down the remaining pathways. If **i6/i9** is formed, this intermediate should also decompose – besides atomic hydrogen loss forming dimethylindenenes (**p5**, **p6**, **p11**, **p12**) – to methylindenenes (**p7/p7'**) at a level of 95% based on our RRKM calculations. Therefore, the non-detection of the methyl loss likely proposes that **p5**, **p6**, **p11**, and/or **p12** are not formed. This can be rationalized considering the inherent barriers to isomerization; intermediate **i1** either decomposes to **p1**, **p2** and/or **p3**, or isomerizes via **i5** to **i2** with the latter decomposing to **p4**. Alternatively, the inherent barriers indicate that intermediate **i3** – if formed – rather eliminates atomic hydrogen or a methyl group yielding **p8**, **p9** and/or **p10** respectively, or isomerizes via **i8** to **i2** with **i2** dissociating to **p4**.

Considering that 1,2-butadiene holds two carbon-carbon double bonds, three carbon atoms are involved in the π -system with charges of -0.26, 0, -0.20.⁴⁵ Therefore, the addition of the 4-tolyl radical to the 1,2-butadiene molecule is likely initiated at the C1 and C3 carbon atoms, with the C1 carbon atom preferred due to the larger cone of acceptance compared to the C3 carbon atom. The failed identification of the methyl loss limits the feasible reaction product(s) even further, as **p3** and **p8** can be ruled out. Products **p1**, **p2**, **p9**, and **p10** can be considered as less important based on the computed reaction energies of only 14-36 kJ mol^{-1} , which are too low to account for the experimental findings (Figure 2). Therefore, we can conclude that the intermediates **i1** and **i3** most likely isomerize to **i2** with the latter yielding **p4** via an atomic hydrogen loss. Further, the

preferential formation of **p4** is fully supported by our RRKM calculations. With respect to the hydrogen loss channels, the computed branching ratio of **p4** is close to 80%, whereas the branching ratios of methylenes (**p7/p7'**) and dimethylenes (**p5, p6, p11, p12**) are 17% and slightly over 1%, respectively, with the other products giving only minor contributions (Table 2). Table 2 also illustrates how the calculated branching ratios depend on the collision energy, E_{col} . At $E_{\text{col}} = 10 \text{ kJ mol}^{-1}$, the direct hydrogen abstraction channels are essentially closed as the collision energy is lower than their barrier heights and they can occur only by tunneling, and hence the major reaction products according to the theoretical calculations should include only **p4** + H (84%) and **p7/p7'** + CH₃ (15%). At $E_{\text{col}} = 20 \text{ kJ mol}^{-1}$, the hydrogen abstraction channels open up and C₄H₅ plus toluene constitute 81% of the total product yield, with **p4** plus hydrogen and **p7/p7'** plus methyl contributing 15% and 3%, respectively. At higher collision energies, the calculated branching ratios exhibit a rather weak dependence on E_{col} , with the hydrogen abstraction products giving 72-69% of the total yield, **p4** plus hydrogen giving 23-25%, and **p7/p7'** plus methyl contributing about 5%.

To conclude, 2-para-tolyl-1,3-butadiene (**p4**) is proposed to be the major product synthesized in the reaction of the 4-tolyl radical with 1,2-butadiene under the single collision conditions. Here, the reaction proceeds via indirect scattering dynamics through the formation of a van-der-Waals complex and is initiated by the addition of the 4-tolyl radical with its radical center to the C1 or C3 carbon atoms of 1,2-butadiene leading to intermediates **i1** (**i3**). The latter isomerize via a de-facto 4-tolyl group migration through bicyclic intermediates **i5** (**i8**) yielding eventually **i2**, which then fragments via hydrogen atom loss from the methyl group of the 1,2-butadiene moiety to 2-para-tolyl-1,3-butadiene (**p4**). Based on the results from the D7-4-tolyl radical reaction with 1,2-butadiene, this mechanism provides compelling evidence that the emitted hydrogen atom

originates from the 1,2-butadiene reactant, but not from the tolyl group. Therefore, our studies demonstrate that the methyl group can present a spectator, but can also be actively involved in the underlying reaction mechanism and hence chemistry. Here, the methyl group at the para position of the phenyl ring seems to be to ‘far away’ to be actively engaged in the chemistry such as hydrogen migration; therefore, this methyl group clearly acts as a spectator and is conserved in the formation of 2-para-tolyl-1,3-butadiene (**p4**). On the other hand, the replacement of a hydrogen atom in the allene reactant by a methyl group has a profound effect on the chemistry since the hydrogen atom emitted from intermediate **i2** is originated from the methyl group adjacent to the C3 carbon atom of the allene moiety. Therefore, this methyl group does not act as a spectator, but is actively engaged in the reaction dynamics of the 4-tolyl radical with 1,2-butadiene.

5. Conclusion

We have conducted the crossed molecular beam reactions of the 4-tolyl radical ($C_6H_4CH_3$) and of the D7-4-tolyl radical ($C_6D_4CD_3$) with 1,2-butadiene (C_4H_6) under single collision conditions at a collision energy of about 54 kJ mol^{-1} . We concluded that 2-para-tolyl-1,3-butadiene (**p4**) likely presents the major reaction product. The reaction proceeds via indirect scattering dynamics through the formation of a van—der-Waals complex and is initiated by the addition of the 4-tolyl radical with its radical center to the C1 or C3 carbon atoms of 1,2-butadiene. The collision complexes isomerize via a de-facto tolyl group migration from the C1 (C3) to the C2 carbon atom of the 1,2-butadiene moiety. The resulting intermediate undergoes unimolecular decomposition via hydrogen atom emission from the methyl group of the 1,2-butadiene moiety through a rather loose exit transition state leading to 2-phenyl-1,3-butadiene (**p4**) suggesting that the methyl group can either act as a spectator (at the phenyl group) or is actively engaged in the underlying chemical dynamics (allene moiety). In strong contrast to the

reaction of the phenyl radical with allene, which leads to the formation of indene,²⁰ the substitution of a hydrogen atom by a methyl group in allene essentially eliminates the formation of bicyclic PAHs such as substituted indenenes in the 4-tolyl plus 1,2-butadiene reaction.

Acknowledgements

This work was supported by the US Department of Energy, Basic Energy Sciences, via grants DE-FG02-03ER15411 (Hawaii) and DE-FG02-04ER15570 (FIU).

References

- (1) Orzechowska, G. E.; Kidd, R. D.; Foing, B. H.; Kanik, I.; Stoker, C.; Ehrenfreund, P. Analysis of Mars Analogue Soil Samples Using Solid-Phase Microextraction, Organic Solvent Extraction and Gas Chromatography/Mass Spectrometry. *Int. J. Astrobiol.* **2011**, *10*, 209-219.
- (2) Bernstein, M. P.; Dworkin, J. P.; Sandford, S. A.; Allamandola, L. J. Ultraviolet Irradiation of Naphthalene in H₂O Ice: Implications for Meteorites and Biogenesis. *Meteorit. Planet. Sci.* **2001**, *36*, 351-358.
- (3) Sarre, P. J.; Miles, J. R.; Scarrott, S. M. Molecular Diffuse Interstellar Band Carriers in the Red Rectangle. *Science* **1995**, *269*, 674-676.
- (4) Allamandola, L. J.; Hudgins, D. M.; Sandford, S. A. Modeling the Unidentified Infrared Emission with Combinations of Polycyclic Aromatic Hydrocarbons. *Astrophys. J.* **1999**, *511*, L115-L119.
- (5) Mansurov, Z. A. Soot Formation in Combustion Processes (Review). *Combust. Explo. Shock+* **2005**, *41*, 727-744.
- (6) Plows, F. L.; Elsila, J. E.; Zare, R. N.; Buseck, P. R. Evidence That Polycyclic Aromatic Hydrocarbons in Two Carbonaceous Chondrites Predate Parent-Body Formation. *Geochim. Cosmochim. Ac.* **2003**, *67*, 1429-1436.
- (7) Granata, S.; Faravelli, T.; Ranzi, E.; Olten, N.; Senkan, S. Kinetic Modeling of Counterflow Diffusion Flames of Butadiene. *Combust. Flame* **2002**, *131*, 273-284.
- (8) Richter, H.; Benish, T. G.; Mazyar, O. A.; Green, W. H.; Howard, J. B. Formation of Polycyclic Aromatic Hydrocarbons and Their Radicals in a Nearly Sooting Premixed Benzene Flame. *P. Combust. Inst.* **2000**, *28*, 2609-2618.
- (9) Hansen, N.; Klippenstein, S. J.; Miller, J. A.; Wang, J.; Cool, T. A.; Law, M. E.; Westmoreland, P. R.; Kasper, T.; Kohse-Hoinghaus, K. Identification of C₅H_x Isomers in Fuel-Rich Flames by Photoionization Mass Spectrometry and Electronic Structure Calculations. *J. Phys. Chem. A* **2006**, *110*, 4376-4388.
- (10) Frenklach, M.; Wang, H. Aromatics Growth Beyond the 1st Ring and the Nucleation of Soot Particles. *Abstr. Pap. Am. Chem. S.* **1991**, *202*, 108-FUEL.
- (11) Frenklach, M. Reaction Mechanism of Soot Formation in Flames. *Phys. Chem. Chem. Phys.* **2002**, *4*, 2028-2037.

- (12) Alkemade, U.; Homann, K. H. Formation of C₆H₆ Isomers by Recombination of Propynyl in the System Sodium Vapor Propynylhalide. *Z. Phys. Chem. Neue. Fol.* **1989**, *161*, 19-34.
- (13) Richter, H.; Howard, J. B. Formation of Polycyclic Aromatic Hydrocarbons and Their Growth to Soot - a Review of Chemical Reaction Pathways. *Prog. Energ. Combust.* **2000**, *26*, 565-608.
- (14) Li, Y. Y.; Zhang, L. D.; Tian, Z. Y.; Yuan, T.; Zhang, K. W.; Yang, B.; Qi, F. Investigation of the Rich Premixed Laminar Acetylene/Oxygen/Argon Flame: Comprehensive Flame Structure and Special Concerns of Polyynes. *P. Combust. Inst.* **2009**, *32*, 1293-1300.
- (15) Li, Y. Y.; Zhang, L. D.; Yuan, T.; Zhang, K. W.; Yang, J. Z.; Yang, B.; Qi, F.; Law, C. K. Investigation on Fuel-Rich Premixed Flames of Monocyclic Aromatic Hydrocarbons: Part I. Intermediate Identification and Mass Spectrometric Analysis. *Combust. Flame* **2010**, *157*, 143-154.
- (16) Fahr, A.; Nayak, A. Kinetics and Products of Propargyl (C₃H₃) Radical Self- Reactions and Propargyl-Methyl Cross-Combination Reactions. *Int. J. Chem. Kinet.* **2000**, *32*, 118-124.
- (17) Lu, M. M.; Mulholland, J. A. PAH Growth from the Pyrolysis of Cpd, Indene and Naphthalene Mixture. *Chemosphere* **2004**, *55*, 605-610.
- (18) Marsh, N. D.; Wornat, M. J.; Scott, L. T.; Necula, A.; Lafleur, A. L.; Plummer, E. F. The Identification of Cyclopenta-Fused and Ethynyl-Substituted Polycyclic Aromatic Hydrocarbons in Benzene Droplet Combustion Products. *Polycycl. Aromat. Comp.* **1999**, *13*, 379-402.
- (19) Gu, X. B.; Kaiser, R. I. Reaction Dynamics of Phenyl Radicals in Extreme Environments: A Crossed Molecular Beam Study. *Acc. Chem. Res.* **2009**, *42*, 290-302.
- (20) Parker, D. S. N.; Zhang, F. T.; Kaiser, R. I.; Kislov, V. V.; Mebel, A. M. Indene Formation under Single-Collision Conditions from the Reaction of Phenyl Radicals with Allene and Methylacetylene-a Crossed Molecular Beam and Ab Initio Study. *Chem.-Asian J.* **2011**, *6*, 3035-3047.
- (21) Parker, D. S. N.; Zhang, F. T.; Kim, Y. S.; Kaiser, R. I.; Landera, A.; Kislov, V. V.; Mebel, A. M.; Tielens, A. G. G. M. Low Temperature Formation of Naphthalene and Its Role in the Synthesis of PAHs (Polycyclic Aromatic Hydrocarbons) in the Interstellar Medium. *P. Natl. Acad. Sci. USA* **2012**, *109*, 53-58.
- (22) Kaiser, R. I.; Parker, D. S.; Zhang, F.; Landera, A.; Kislov, V. V.; Mebel, A. M. PAH Formation under Single Collision Conditions: Reaction of Phenyl Radical and 1,3-Butadiene to Form 1,4-Dihydronaphthalene. *J Phys Chem A* **2012**, *116*, 4248-4258.

- (23) Zhang, T. C.; Zhang, L. D.; Hong, X.; Zhang, K. W.; Qi, F.; Law, C. K.; Ye, T. H.; Zhao, P. H.; Chen, Y. L. An Experimental and Theoretical Study of Toluene Pyrolysis with Tunable Synchrotron Vuv Photoionization and Molecular-Beam Mass Spectrometry. *Combust. Flame* **2009**, *156*, 2071-2083.
- (24) da Silva, G.; Cole, J. A.; Bozzelli, J. W. Kinetics of the Cyclopentadienyl Plus Acetylene, Fulvenallene + H, and 1-Ethynylcyclopentadiene Plus H Reactions. *J. Phys. Chem. A* **2010**, *114*, 2275-2283.
- (25) Smith, R. A Direct Mass Spectrometric Study of the Mechanism of Toluene Pyrolysis at High Temperatures. *J. Phys. Chem.* **1979**, *83*, 1553-1563.
- (26) Parker, D. S. N.; Dangi, B. B.; Kaiser, R. I.; Jamal, A.; Ryazantsev, M. N.; Morokuma, K.; Korte, A.; Sander, W. An Experimental and Theoretical Study on the Formation of 2-Methylnaphthalene (C₁₁H₁₀/C₁₁H₃D₇) in the Reactions of the Para-Tolyl (C₇H₇) and Para-Tolyl-D₇ (C₇D₇) with Vinylacetylene (C₄H₄). *J. Phys. Chem. A* **2014**.
- (27) Kaiser, R. I.; Maksyutenko, P.; Ennis, C.; Zhang, F. T.; Gu, X. B.; Krishtal, S. P.; Mebel, A. M.; Kostko, O.; Ahmed, M. Untangling the Chemical Evolution of Titan's Atmosphere and Surface—from Homogeneous to Heterogeneous Chemistry. *Faraday Discuss.* **2010**, *147*, 429-478.
- (28) Dames, E.; Wang, H. Isomerization Kinetics of Benzylic and Methylphenyl Type Radicals in Single-Ring Aromatics. *P. Combust. Inst.* **2013**, *34*, 307-314.
- (29) Ichimura, T.; Mori, Y.; Shinohara, H.; Nishi, N. 3 Dissociation Channels for P-Dichlorobenzene Excited at 193-Nm in Molecular-Beams. *Chem. Phys. Lett.* **1985**, *122*, 55-58.
- (30) Ichimura, T.; Mori, Y.; Shinohara, H.; Nishi, N. Photofragmentation of Chlorotoluenes and Dichlorobenzenes: Substituent Effects on the Dissociation Mechanism, and Angular Distribution of the Cl Fragment. *J. Chem. Phys.* **1997**, *107*, 835-842.
- (31) Kochi, J. K. The Mechanism of the Sandmeyer and Meerwein Reactions. . *J. Am. Chem. Soc.* **1957**, *79*, 2942-2948.
- (32) Stephens, P. J.; Devlin, F. J.; Chabalowski, C. F.; Frisch, M. J. Ab-Initio Calculation of Vibrational Absorption and Circular-Dichroism Spectra Using Density-Functional Force-Fields. *J. Phys. Chem.* **1994**, *98*, 11623-11627.
- (33) Baboul, A. G.; Curtiss, L. A.; Redfern, P. C.; Raghavachari, K. Gaussian-3 Theory Using Density Functional Geometries and Zero-Point Energies. *J. Chem. Phys.* **1999**, *110*, 7650-7657.

- (34) Curtiss, L. A.; Raghavachari, K.; Redfern, P. C.; Baboul, A. G.; Pople, J. A. Gaussian-3 Theory Using Coupled Cluster Energies. *Chem. Phys. Lett.* **1999**, *314*, 101-107.
- (35) Curtiss, L. A.; Raghavachari, K.; Redfern, P. C.; Rassolov, V.; Pople, J. A. Gaussian-3 (G3) Theory for Molecules Containing First and Second-Row Atoms. *J. Chem. Phys.* **1998**, *109*, 7764-7776.
- (36) Frisch, M. J., et al. *Gaussian 09, Revision A.1*, Gaussian, Inc: Wallingford CT, 2009.
- (37) Werner, H.-J.; Knowles, P. J.; Kinizia, G.; Manby, F. R.; Schutz, M.; Celani, P.; Korona, T.; Lindh, R. *Molpro, Version 2010.1, a Package of Ab Initio Programs*, MOLPRO, version 2010.1.; 2010.
- (38) Eyring, H.; Lin, S. H.; Lin, S. M., *Basis Chemical Kinetics*. Wiley: New York, 1980.
- (39) Kaiser, R. I.; Parker, D. S. N.; Goswami, M.; Zhang, F.; Kislov, V. V.; Mebel, A. M.; Aguilera-Iparraguirre, J.; Green, W. H. Crossed Beam Reaction of Phenyl and D5-Phenyl Radicals with Propene and Deuterated Counterparts-Competing Atomic Hydrogen and Methyl Loss Pathways. *Phys. Chem. Chem. Phys.* **2012**, *14*, 720-729.
- (40) Maity, S.; Parker, D. S. N.; Dangi, B. B.; Kaiser, R. I.; Fau, S.; Perera, A.; Bartlett, R. J. A Crossed Molecular Beam and Ab-Initio Investigation of the Reaction of Boron Monoxide (Bo; X-2 Sigma(+)) with Methylacetylene (Ch3cch; X(1)a(1)): Competing Atomic Hydrogen and Methyl Loss Pathways. *J. Phys. Chem. A* **2013**, *117*, 11794-11807.
- (41) Kaiser, R. I.; Maity, S.; Dangi, B. B.; Su, Y. S.; Sun, B. J.; Chang, A. H. H. A Crossed Molecular Beam and Ab Initio Investigation of the Exclusive Methyl Loss Pathway in the Gas Phase Reaction of Boron Monoxide (BO; X²Σ⁺) with Dimethylacetylene (CH₃CCCH₃; X¹A_{1g}). *Phys. Chem. Chem. Phys.* **2014**, *16*, 989-997.
- (42) Levine, R. D., *Molecular Reaction Dynamics*. Cambridge University Press: Cambridge, UK, 2005.
- (43) Steinfeld, J. I.; Francisco, J. S.; Hase, W. L., *Chemical Kinetics and Dynamics*. 2nd ed.; Prentice Hall: New Jersey, 1999.
- (44) Kaiser, R. L.; Parker, D. S. N.; Zhang, F.; Landera, A.; Kislov, V. V.; Mebel, A. M. Pah Formation under Single Collision Conditions: Reaction of Phenyl Radical and 1,3-Butadiene to Form 1,4-Dihydronaphthalene. *J. Phys. Chem. A* **2012**, *116*, 4248-4258.
- (45) Gu, X. B.; Zhang, F. T.; Kaiser, R. I.; Kislov, V. V.; Mebel, A. M. Reaction Dynamics of the Phenyl Radical with 1,2-Butadiene. *Chem. Phys. Lett.* **2009**, *474*, 51-56.

Table 1: Peak velocities (v_p), speed ratio (S), collision energy (E_c), and corresponding center-of-mass angles (Θ_{CM}) of the primary and secondary beams.

	v_p (ms ⁻¹)	S	E_c (kJ mol ⁻¹)	Θ_{CM}
C ₄ H ₆ (1,2-butadiene)	760 ± 20	7.5 ± 0.2		
C ₇ H ₇ (4-tolyl)	1640 ± 40	8.0 ± 0.5	53.4 ± 2.0	15.0 ± 0.9
C ₇ D ₇ (D7-4-tolyl)	1644 ± 30	8.7 ± 0.5	55.2 ± 1.9	14.8 ± 0.8

Table 2: Branching ratios of the p-tolyl plus 1,2-butadiene reaction at various collision energies.

	E_{col} , kJ mol ⁻¹					
	10	20	30	50	54	60
p1	0.00	0.00	0.00	0.00	0.00	0.00
p2	0.00	0.00	0.00	0.00	0.00	0.01
p3	0.01	0.01	0.02	0.09	0.11	0.16
p5	0.21	0.04	0.07	0.08	0.08	0.08
p6	0.40	0.09	0.14	0.17	0.17	0.18
p7	9.58	1.91	2.77	2.90	2.87	2.81
p8	0.01	0.01	0.02	0.07	0.09	0.11
p9	0.00	0.00	0.00	0.00	0.00	0.00
p10	0.00	0.00	0.00	0.00	0.00	0.00
p4	84.35	15.24	22.69	24.68	24.50	24.13
p7'	5.18	1.34	2.14	2.43	2.44	2.42
p11	0.11	0.03	0.05	0.06	0.06	0.07
p12	0.14	0.04	0.07	0.09	0.10	0.10
CH ₃ CCCH ₂	0.00	28.18	25.68	23.98	23.82	23.63
CH ₂ CHCCH ₂	0.00	33.38	28.45	25.25	24.95	24.60
CH ₃ CHCCH	0.00	19.73	17.89	20.19	20.80	21.71

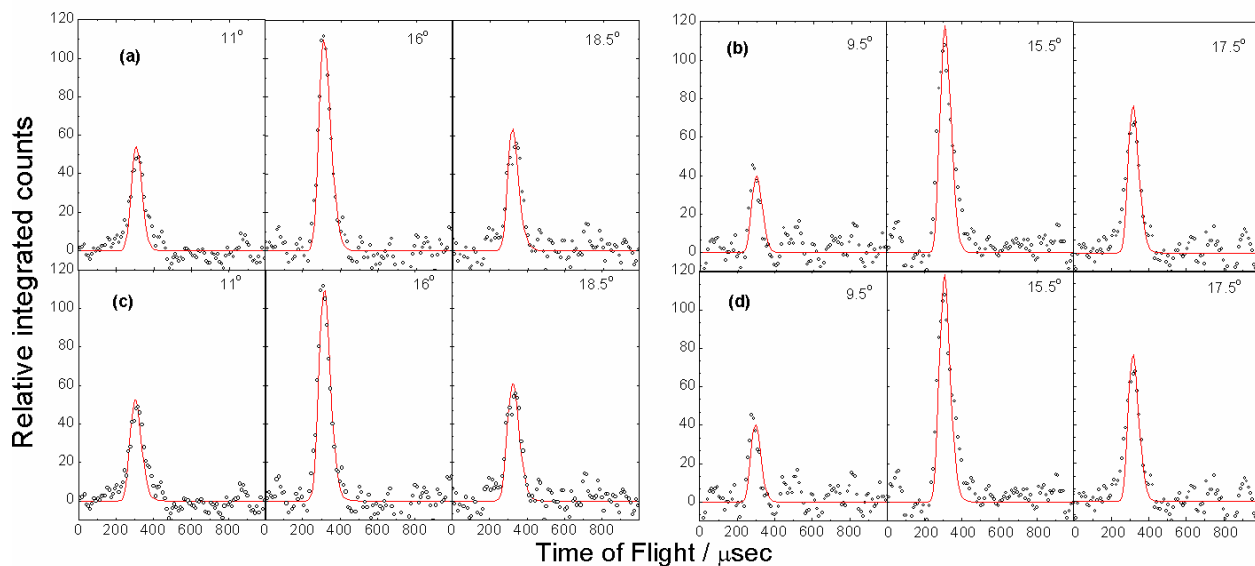


Figure 1: Selected time-of-flight (TOF) spectra recorded at mass-to-charge (m/z) ratios of 144 [$C_{11}H_{12}^+$, (a)/(c)] and 151 [$C_{11}D_7H_5^+$, (b)/(d)] for the reactions of the 4-tolyl radical ($C_6H_4CH_3$) and the D7-4-tolyl radical [$C_6D_4CD_3$] with 1,2-butadiene [C_4H_6] fit with low reaction exoergiciencies of 75 kJ mol^{-1} [(a)/(b)] and higher reaction exoergiciency of 150 kJ mol^{-1} [(c)/(d)], respectively. The circles represent the experimental data points, while the solid lines represent the fits.

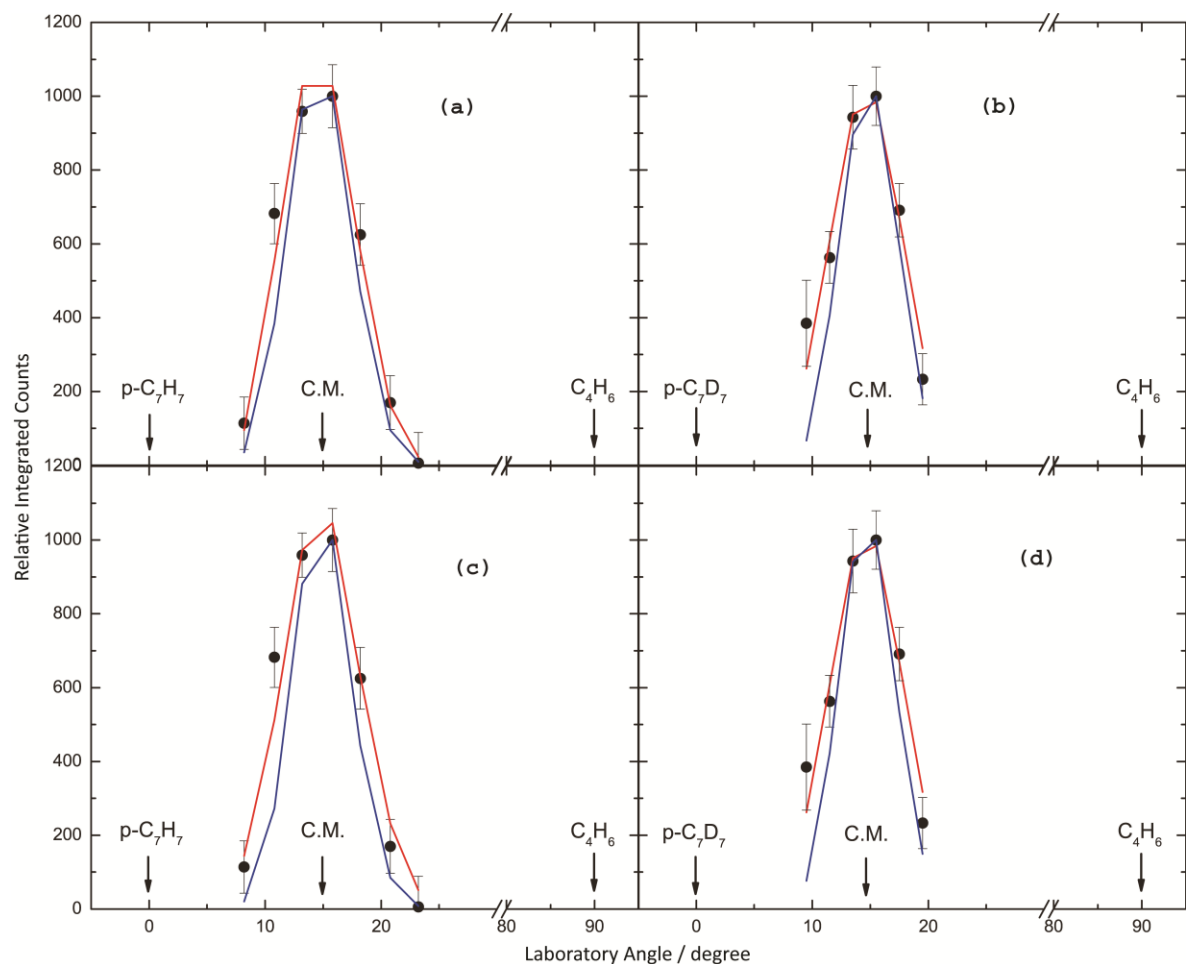


Figure 2: Laboratory (LAB) angular distributions of signal at m/z of 144 [$C_{11}H_{12}^+$, (a)/(c)] and 151 [$C_{11}D_7H_5^+$, (b)/(d)], for the reactions of the 4-methylphenyl radical ($C_6H_4CH_3$; X^2A_1) and D7-4-methylphenyl radical ($C_6D_4CD_3$; X^2A_1) with 1,2-butadiene (C_4H_6 ; X^1A'), respectively. The solid circles depict the experimental data and the red solid lines represent the calculated best fits. The blue lines represent the calculated distribution assuming a low reaction exoergicity of 30 kJ mol^{-1} . The best fit red lines were obtained at a low reaction exoergicity of 75 kJ mol^{-1} [(a)/(b)] and at a high reaction exoergicity of 150 kJ mol^{-1} [(c)/(d)], respectively.

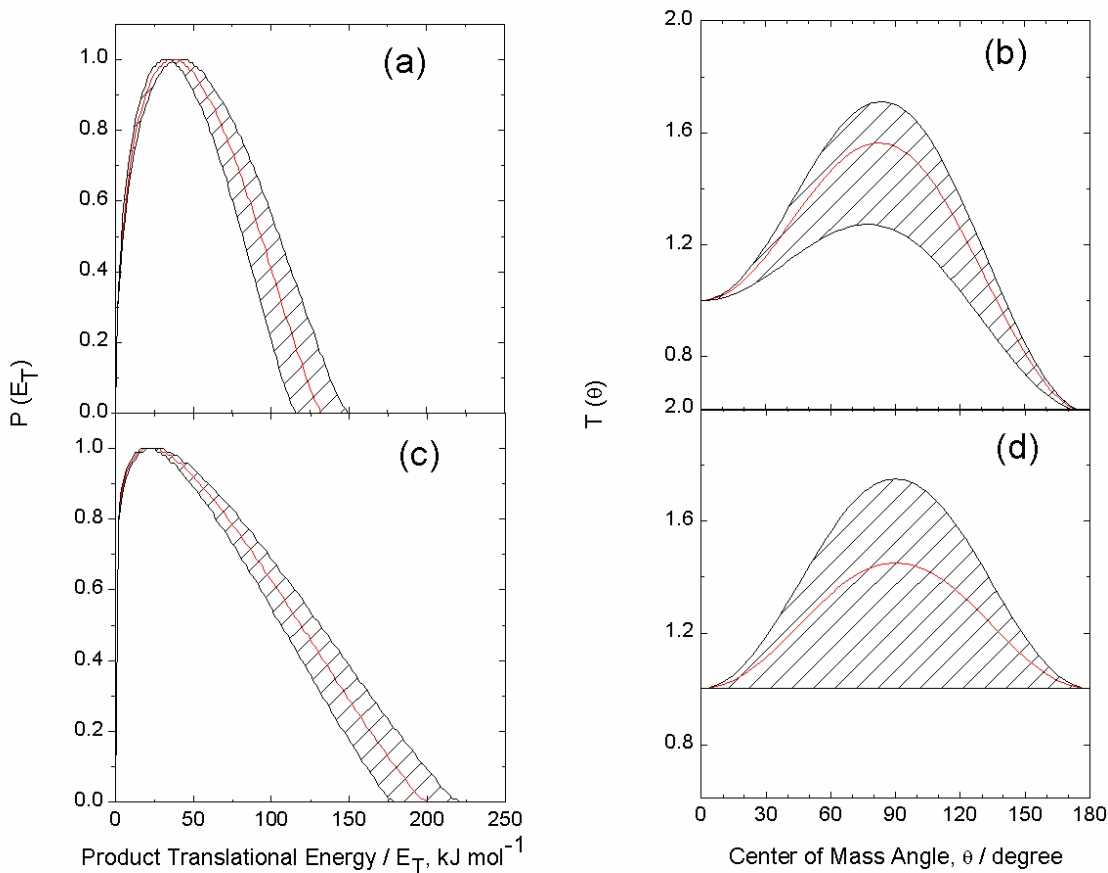


Figure 3: Center-of-mass translational energy distributions [(a)/(c)] and angular distributions [(b)/(d)] exploited to fit the laboratory data of the 4-tolyl/D7-4-tolyl radical with 1,2-butadiene reactions via a single channel reaction leading to $\text{C}_{11}\text{H}_{12}$ and $\text{C}_{11}\text{D}_7\text{H}_5$ products via atomic hydrogen losses at a low reaction exoergicity of 75 kJ mol^{-1} [(a)/(b)] and at a high reaction exoergicity of 150 kJ mol^{-1} [(c)/(d)], respectively. The hatched areas represent the error limits.

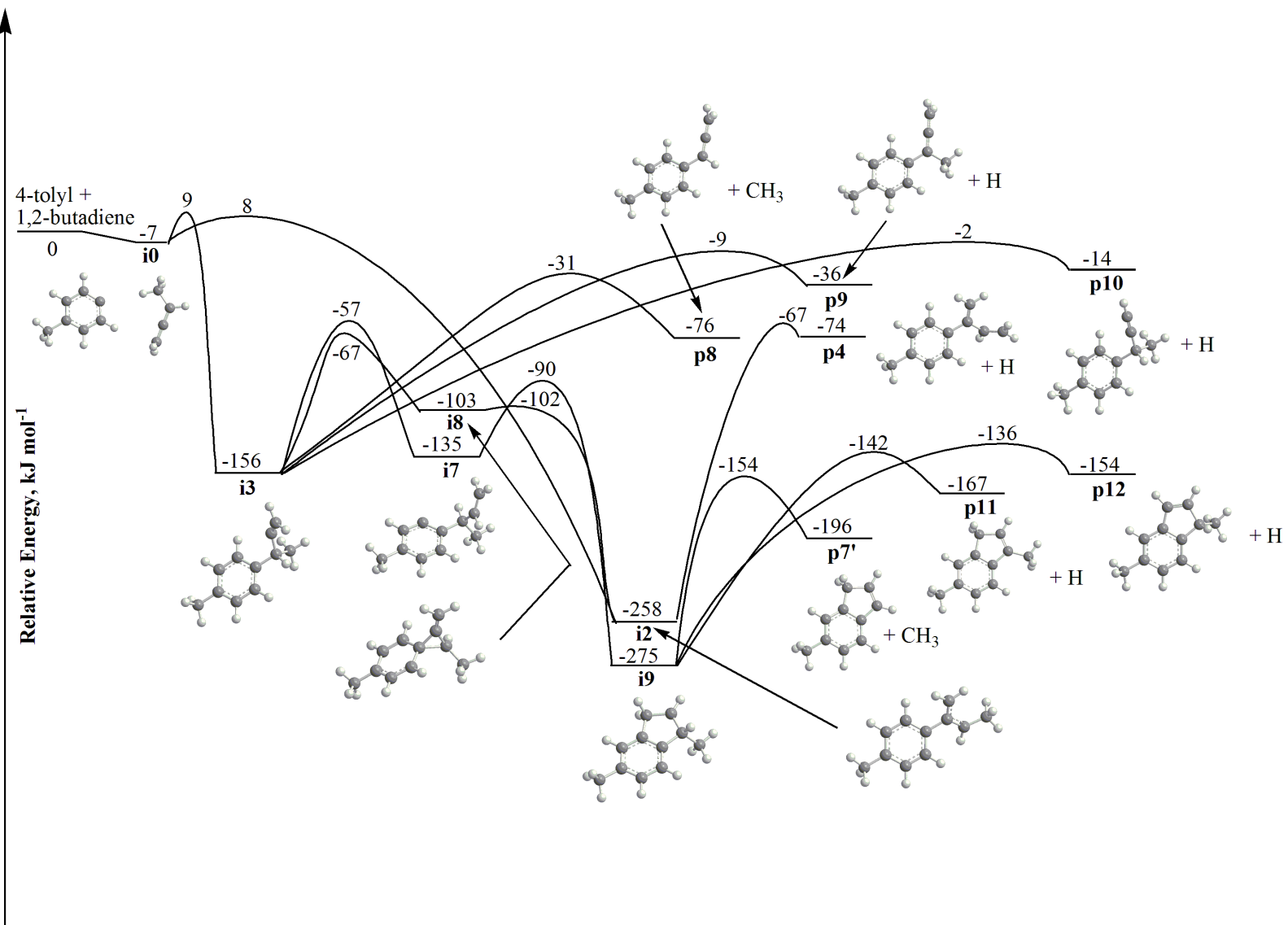


Figure 5: Potential energy surface for the reaction of the 4-tolyl radical addition to the C3 and C2 carbon atoms of 1,2-butadiene calculated at the G3(MP2,CC)//B3LYP/6-311G** level of theory. All relative energies are given in kJ mol^{-1} .

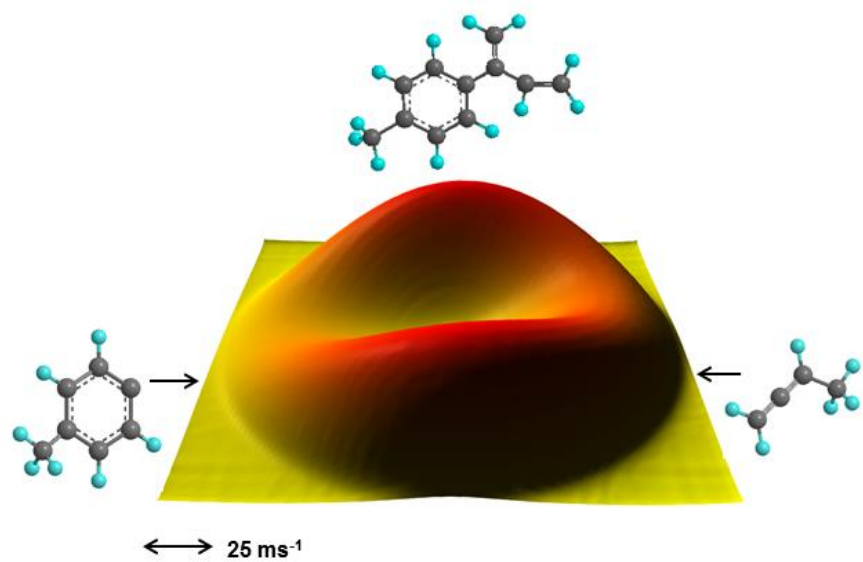


Figure: TOC